A Two-Dimensional Analysis of the Effect of a Rotating Cylinder on an Inverted Aerofoil in Ground Effect.

S. Diasinos[1], T.J. Barber[1], E. Leonardi[1] and S.D. Hall[1]

[1]School of Mechanical & Manufacturing Engineering
The University of New South Wales, NSW, 2052 AUSTRALIA

Abstract

The effect of a front wheel behind a front wing (on an open wheel racing car) was studied using Computational Fluid Dynamics (CFD). Results are presented for a 2D analysis conducted on an aerofoil and cylinder. CFD models are used to compare and demonstrate the effect that these two objects have on each other, when operating in close proximity. From the CFD analysis it was determined that the aerofoil generates lift, instead of the desired downforce in several of the configurations studied and only in certain positions is the aerofoil beneficial. This may explain the reduction in the front wing span that teams adopted after the Formula One (F1) regulation changes for the 1998 season.

Introduction

In modern open wheeler racing cars, aerodynamics plays a critical role in determining the competitiveness of the vehicle. This is most evident in F1 where teams spend a large portion of their budget tailoring and perfecting their vehicles aerodynamics in an attempt to obtain a crucial advantage over their opposition. As a result, research conducted by teams is rarely made public. The majority of research that has been published on open wheeler aerodynamics, until this point, has focused on individual components studied on their own. This has included aerofoils and wings [7], cylinders [5], wheels [4] and diffusers [6]. Several publications have also presented a general overview of the aerodynamic aspects of an open wheeler racing car [3].

This paper attempts to explain the effect and interaction that the front wing and wheel (two common components of all open wheeler racing cars), have on each other. A 2D CFD analysis of a Cylinder and Aerofoil (A&C) was the preliminary study for this complex aerodynamic interaction. In the near future, a 2D experimental analysis will be used to verify the results presented in this paper. Later studies will also include a 3D CFD analysis and a 3D experimental analysis. Experimental techniques that will be used include flow visualisation and advanced laser diagnostics (LDV and PIV).

CFD Model

A commercially available CFD package (Fluent 6.1.22) was used. The model consisted of an inverted NACA 4412 aerofoil in front of a circle in contact with the ground, as depicted in figure 1. An extensive verification study was conducted prior to the CFD model being used [2] which included grid refinement. The total number of elements in the CFD model ranged from 240000 to 260000. Grids that utilised up to 550000 elements were found to have no significant improvement on the accuracy of the model. Similar studies were also undertaken ensuring that the results obtained were independent of the positions of the boundaries and that of the convergence levels used.

During the CFD modelling results were obtained at angles within the range of -6° to 24° in increments of 3°. Results were obtained at ground clearance values of 0.05c (chord), 0.13c, 0.25c and 0.50c. All results presented here are for a cylinder separation of 0.13c as defined by figure 1. The circle diameter was kept the

same as the aerofoil chord. This is also the reference length that was used for the Reynolds number, and lift and drag coefficients. All the results for the A&C were obtained at Reynolds number of 4.1x10^5, ensuring turbulent flow.
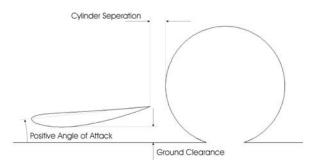

Figure 1. Parameters adjusted during analysis

The cylinder and aerofoil surfaces were modelled as smooth walls (no roughness). Even though this may not accurately depict the surface of a tyre, this is an accurate representation of the surface of the experimental apparatus that will be used to verify the CFD. A k-epsilon, RNG turbulence model was used, with enhanced, pressure gradient wall treatment so that the boundary layer over the aerofoil and cylinder could be monitored. The RNG turbulence model was chosen as it is an improved version of the standard k-epsilon turbulence model and is better suited to small levels of turbulence.

Lift values were obtained for a NACA 4412 aerofoil in free stream at a Reynolds number of 3.0x10^6 using the same CFD model for a range of angles of attack of -6° to 18° and these were found to agree within 5% to the results published by Abott &Von Doenhoff [1]. Drag data followed the correct trend, however the actual error was larger.

Results
Aerofoil Pressure Coefficients

From figure 2, it can be seen that the pressure beneath an inverted aerofoil in ground effect reduces as the aerofoil approaches the ground. The camber in the aerofoil allows the air flow to be
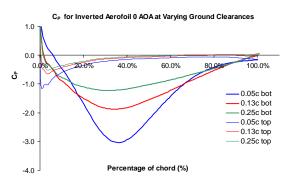

Figure 2. Aerofoil Coefficient of Pressure plots for Aerofoil bottom side at different Ground Clearances for an 0° angle of attack.

accelerated between the aerofoil and the ground. The rear of the aerofoil acts as a diffuser, the lower pressure region behind the aerofoil assisting with increasing the speed of the airflow between the aerofoil and the ground. Both these factors contribute to lowering the pressure beneath the aerofoil and this is the reason that an inverted wing in ground effect has improved performance in comparison to an aerofoil in free stream. As the angle of attack is increased, the lift also increases until stall is achieved at a much smaller angle in comparison to the free stream aerofoil. Zerihan and Zhang[7] obtained similar results during their experimental analysis explaining why an inverted aerofoil experiences improved performance near the ground.

Cylinder Pressure Coefficients

Figure 3 shows that there was a large pressure acting at the base of the cylinder near the front of the contact patch, as well as behind the rear contact patch. Over the top of the cylinder, a lower pressure exists and because of this, a spinning cylinder in contact with the ground generates lift.
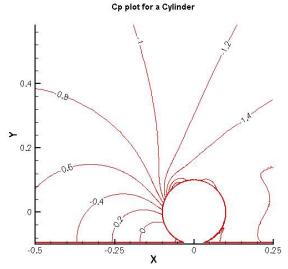

Figure 3. Coefficient of Pressure Contour plot for a cylinder.

This high pressure region is not confined to just the front contact patch of the cylinder, but also extends forward. Another important feature that is evident from the Coefficient of Pressure contour plot (fig 3) is the separation point that is located slightly forward of the top of the cylinder.

Aerofoil and Cylinder Pressure Coefficients

The high pressure region forward of the front contact patch that was discussed earlier (figure 3) was also evident in results obtained for the aerofoil and cylinder case (figure 4). This high pressure region acts on the bottom surface of the aerofoil and for this reason the aerofoil was generating lift as opposed to the desired downforce. This could potentially be the reason why the front wings on F1 cars have had a reduced span after the regulation changes imposed for the 1998 season. The regulation changes required that the maximum width of the car be reduced from 200cm to 180cm and this would have further increased the interaction between the front wheel and wing.

Similarly, this is the reason that the aerofoil was experiencing a forward force, or a negative drag, in most positions tested in the presence of the cylinder. As the angle of attack was increased, more area was exposed to the high pressure region generated

forward of the cylinder contact patch and hence the lift and the negative drag increased in magnitude (figure 4).

Changing the angle of attack of the aerofoil has relatively little difference on the pressure generated at the contact patch, as this is always a stagnated flow. This is not the case for the front of the cylinder where the pressure decreases as the aerofoil angle of attack was increased. For this reason the drag of the cylinder was affected more by the aerofoil angle of attack than the lift generated by the cylinder was.
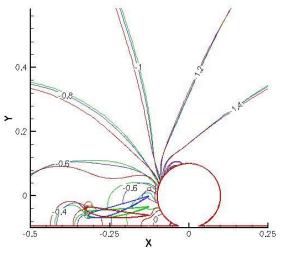

Figure 4. Aerofoil and Cylinder Coefficient of Pressure contour plot a various angles of attack for the aerofoil at a ground clearance of 0.13c

Wing Lift Results

The lift curve slope obtained for an inverted wing in ground effect on its own, using the CFD model is compared to the experimental results obtained by Zerihan and Zhang[7] in figure 5. As the angle of attack is increased, the down force generated increases until the wing reaches stall. After this occurs, the downforce generated by the aerofoil reduces steadily. As the aerofoil ground clearance is reduced, the stall angle also reduces. These trends are evident in both the results obtained using the CFD model and also those obtained by Zerihan and Zhang[7]. The values for the coefficient of lift and the stall positions differ slightly because two different aerofoil have been used in the two studies since the coordinates of the aerofoil used by Zerihan and
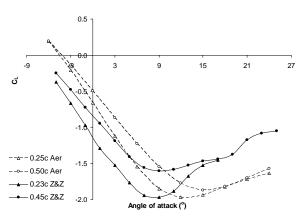

Figure 5. Lift curve slope comparing results by Zerihan and Zhang[7] (Z&Z) with those obtained using the Aerofoil model (Aer).

Zhang were not included in this reference and it is an aerofoil developed by an F1 team.

The lift curve slope for the aerofoil varied significantly when placed in close proximity to a spinning cylinder. Figure 6 shows the lift curve slope for a NACA 4412 aerofoil with a separation of 0.13c from the cylinder at different ground clearances. For the lower ground clearances the lift curve slope is reversed compared too that of the aerofoil working in ground effect on its own. As the aerofoil is raised further from the ground, the lift curve slope gradually changes direction until it is in the same direction as the aerofoil on its own. When comparing the lowest ground clearance for the two cases, the greatest downforce is generated at an angle of attack of 12° for the aerofoil on its own and at the greatest negative angle of attack tested (-6°) for the aerofoil and cylinder.
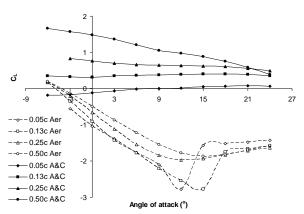

Figure 6. Lift curve slope comparing aerofoil on its own and aerofoil with cylinder separation of 0.13c

The magnitude of the downforce generated by the aerofoil in close proximity to the cylinder is also affected. The greatest level of downforce was still generated when the aerofoil was in the closest proximity to the ground tested, but the magnitude was small in comparison to the aerofoil on its own. As the aerofoil ground clearance increases, the aerofoil begins to generate lift instead of downforce.

Wing Drag Results
The drag that the aerofoil develops is also affected by the presence of the cylinder. The aerofoil on its own has a steadily increasing drag as the angle of attack is increased up until the stall position. For the lower heights, the drag drops after the stall position and then continues to rise. The two greater ground clearances tested on the other hand, continued to rise and no drop in drag was evident after stall was achieved. As the aerofoil ground clearance is increased, the drag magnitude for all angles of attack reduces.

In the presence of the cylinder, the aerofoil drag decreases with an increase in angle of attack. As can be seen from figure 7, this trend is the opposite of that obtained for the aerofoil on its own, at similar ground clearances. The drag values for all the positive angles tested were also found to be negative implying that the high pressure region forward of the cylinder is pushing the aerofoil forward in most positions tested.

At the lowest ground clearance tested, the angle of attack had little change on the drag of the aerofoil. As the ground clearance was increased for the aerofoil, this becomes more pronounced,

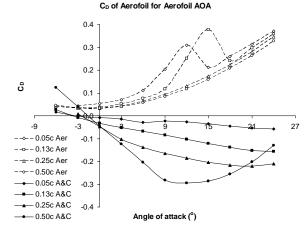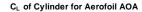but the minimum drag value was obtained at a lower AOA

Figure 7. Cd comparing aerofoil in ground effect (Aer) with aerofoil in the presence of a cylinder (A&C) at different ground clearances

Cylinder Lift Results
The cylinder lift varied little as the aerofoil angle of attack was varied at the lowest ground clearance tested. As the ground clearance was increased, a change in the angle of attack of the aerofoil would result in a more significant change to the cylinder lift. These results are shown in figure 8. The presence of the cylinder drastically reduces the lift generated by the cylinder, as represented by the broken line in figure 8.

The results obtained at the three lowest ground heights all follow similar trends, were the maximum lift generated by the cylinder occurs when the aerofoil has an angle of attack of approximately 12°. When the aerofoil has a much greater clearance of 0.5c, at the same angle of attack, the minimum lift case occurs. At the larger ground clearance as the angle of attack of the aerofoil is increased, a larger amount of air is deflected away from the cylinder and this reduces the speed of the air over the top of the cylinder and therefore the lift of the cylinder. In the lower positions, no angle of attack is large enough to create a similar effect and for this reason the trend is reversed for the larger ground clearance.
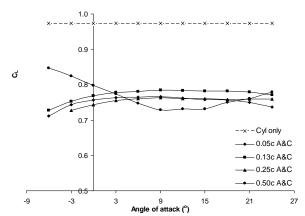

Figure 8. Lift coefficients of the cylinder on its own (Cyl) and with an aerofoil in front (A&C) at different ground clearances and angles of attack of the aerofoil.

Cylinder Drag Results
The effect that the aerofoil angle of attack has on the cylinder becomes more pronounced as the aerofoil ground clearance is

increased. The drag curves shown in figure 9 exhibit opposite trends to that of the aerofoil drag discussed previously (figure 7). While the aerofoil drag values decrease with an increasing angle of attack and an increase in the ground clearance, the cylinder experiences an increase in drag with increasing aerofoil ground clearance and angle of attack. Only for a small number of positions tested did the cylinder have a reduced drag in comparison to the cylinder on its own. This is represented in figure 9.
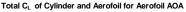
C_D of Cylinder for Aerofoil AOA

Figure 9. Drag coefficients of the cylinder on its own (Cyl) and the cylinder in the presence of the aerofoil (A&C) at different ground clearances and angles of attack for the aerofoil.

Total Lift and Drag Results

Also of great interest was how the two components performed together as both the wing and the wheel contribute to the lift and drag generated by a racing car. For this reason, minimising the lift and drag of both is more important than reducing the lift or drag for each individual component. These results have been included in this paper as the optimum compromise between drag and lift varies depending on the characteristics of the track that the open wheeler will compete at.

The total lift of these two objects can be controlled by careful placement of the aerofoil relative to the cylinder. To minimize the lift generated by the two bodies combined, it was found that the best combination of angle of attack and ground clearance was at the lowest ground clearance and the most negative angle of attack tested (0.05c, -6°). This can be seen in figure 10 where the broken line represents the lift that the cylinder would experience

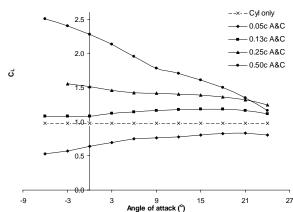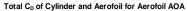**Total C_L of Cylinder and Aerofoil for Aerofoil AOA**

Figure 10. Total lift for aerofoil and cylinder compared to the cylinder on its own.

on its own. In this position it is possible to reduce the lift generated by the cylinder alone by approximately 50% by placing the aerofoil forward of the cylinder and for a small drag penalty.

The total drag result for a given ground clearance did not change significantly with a changing angle of attack. The only significant change occurs with a change in the aerofoil ground clearance. In order to minimize the drag of the two objects it would be necessary to increase the ground clearance of the aerofoil. The best result obtained, amongst the positions tested, for minimizing the drag was found to occur at a ground clearance of 0.5c and an angle of attack of -6°. Unfortunately the same position would result in a significant increase in lift.

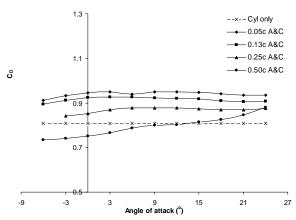**Total C_D of Cylinder and Aerofoil for Aerofoil AOA**

Figure 11. Total drag for aerofoil and cylinder (A&C) at different ground clearances for the aerofoil compared to the cylinder (Cyl) on its own.

Conclusion

This analysis suggests that the cylinder has a substantial affect on the performance of the aerofoil. The main reason for the significant change found for the aerofoil performance in the presence of the cylinder was due to the large pressure region that is created forward of the contact patch of the cylinder. While the analysis thus far has only been conducted using CFD, in the near future experimental results will be used to verify the CFD results. The results obtained during this analysis imply that it would be beneficial to continue this research so that it may include a 3D CFD and experimental model of a finite width wing and wheel.

References

[1]. Abbot, I.H. &Von Doenhoff, A.E., Theory of Wing sections

[2]. AIAA, Guide for Verification and Validation of Computational Fluid Dynamics Simulations *AIAA G-077-1998*

[3]. Dominy, R.G., Aerodynamics of Grand Prix Cars, *Proceedings of the Institution of Mechanical engineers, Part D: Journal of Automobile Engineering, Vol. 206, no.D4, 1992, pp. 267-274*

[4]. Fackrell, J.E., & Harvey., The Aerodynamics of an Isolated Road Wheel, *No. 8 Proceedings of the Second Symposium on Aerodynamics of Sports and Competition Automobiles, collection of AIAA papers published by western Periodicals Co., North Hollywood, CA, 1975*

[5]. Mittal, S. & Kumar, B., Flow Past a Rotating Cylinder, *J. Fluid Mech (2003), Vol 476 pp. 303-334*

[6]. Sovran, G., and Klomp, E.D., Experimentally Determined Optimum Geometries for Rectilinear Diffusers with rectangular, Canonical or Annular Cross-Section, *Fluids Mechanics of internal Flows, Elsevier Publishing Co., N.Y., 1967 pp. 270-319.*

[7]. Zerihan, J. & Zhang, J., Aerodynamics of a Single Element Wing in Ground Effect, *Journal of Aircraft, Vol 37, No 6, pp.1058 – 1064, November-December 2000*